NUCLEAR REACTIONS AND NEUTRINOS IN STELLAR EVOLUTION

W. DAVID ARNETT
Dept. of Astronomy, University of Texas, Austin, Tex., U.S.A.

Much of the material discussed in this review represents a summary of some chapters in a monograph I am writing (Arnett, 1974); a more detailed discussion will be found there.

1. Neutrinos

A fundamental question for astrophysics is whether or not there exists a direct $e-\nu$ coupling in the weak interaction. As first emphasized by Pontecorvo (1959) this would imply efficient cooling processes for late stages of stellar evolution. Such an interaction is predicted by the conserved vector current (CVC) theory of weak interactions proposed by Feynman and Gell-Mann (1958). Dicus (1972) has shown that the theory of leptons of Stephen Weinberg (1971) gives cooling processes similar to those predicted by CVC, but with an uncertainty related to the precise value of the mass of the charged vector (W) meson which mediates the interaction.

Beaudet *et al.* (1967) have used CVC theory and numerically evaluated the composition-independent neutrino emission rates; they give analytic fits for the rate of radiation of energy by these processs. Also using CVC theory, Festa and Ruderman (1969) have examined neutrino-pair bremsstrahlung in a plasma consisting of degenerate electrons and nondegenerate ions; this process is probably important at high density and low temperature.

Figure 1 displays the rate of energy loss due to neutrino emission per gram, ε_ν, multiplied by the number of nucleons per electron, μ_e. This quantity $\mu_e\varepsilon_\nu$ is convenient because it is independent of μ_e. In Figure 1, $\mu_e\varepsilon_\nu$ is plotted vs the logarithm to base 10 of ϱ/μ_e where ϱ is the usual nucleon mass density. The curves are parametrized by temperature T, and labeled by $\log T(\mathrm{K})$. The solid lines refer to the Beaudet *et al.* rates; the dashed curves represent the Festa-Ruderman rate for a gas of pure ^{12}C.

At the high densities encountered in the late stages of stellar evolution, electron capture processes can become important. In the *Urca process* a nucleus alternatively captures an electron and undergoes a beta decay, meanwhile emitting a neutrino and an antineutrino. Thus a cyclic (but nonreversible) process occurs. In *neutronization* increasing density induces electron capture and causes a diminution in the number of electrons per nucleon present in the plasma. In general this is a noncylic process. Both types of process are currently under active study. In both cases the nature of the process depends upon previous evolution. For the Urca process, the abundance of Urca-active nuclei is of vital importance, and depends upon previous thermonuclear processing which can destroy or produce such nuclei. Neutronization might be less sensitive to previous evolution than the Urca process, but it too depends upon the

Tayler (ed.), Late Stages of Stellar Evolution, 1–14. *All Rights Reserved, Copyright © 1974 by the IAU.*

https://doi.org/10.1017/S0074180900017617 Published online by Cambridge University Press

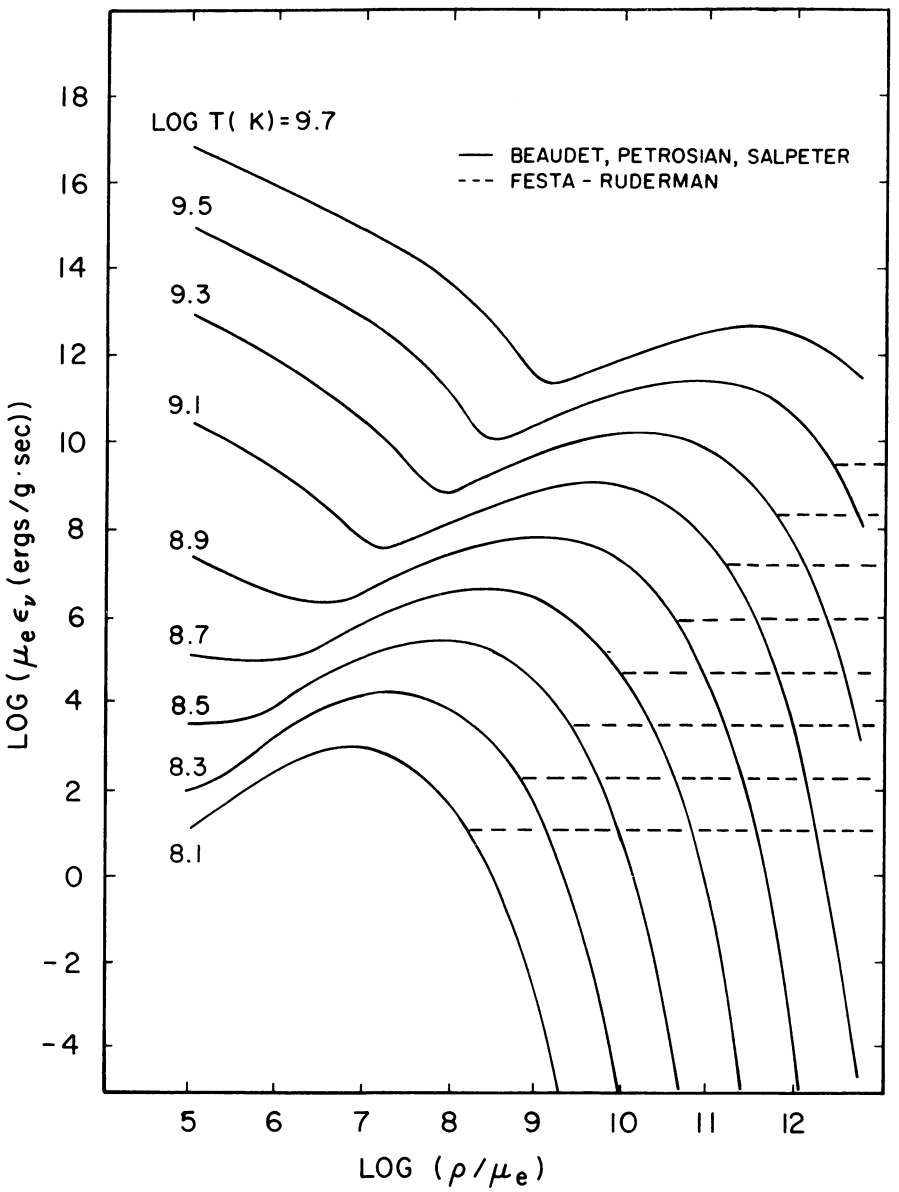

Fig. 1. Energy losses due to neutrino emission, as predicted by conserved vector current (CVC) theory.

composition, size and nature of the stellar core. Since these topics will be discussed in some detail in other papers (see especially those by Paczyński and by Imshennik and Nadyozhin), I will end regretfully my discussion of this fascinating and important topic here.

https://doi.org/10.1017/S0074180900017617 Published online by Cambridge University Press

2. An Overview of the Stages of Thermonuclear Burning

The thermonuclear evolution of stellar matter may be thought of as consisting of a sequence of stages, in which the ashes of one stage become the fuel of the next. To describe such a sequence the stellar evolutionist must know at least two things: (1) the *rate of energy generation* by the thermonuclear consumption of a given fuel, and (2) the *composition* of the ashes which will become the fuel for the next stage. The evolutionary change in stellar composition is an initial-value problem; in general errors can amplify with successive evolution. Consequently it is vital to accurately represent the earlier burning stages if we wish to explore the later ones.

By far the vast bulk of stellar evolutionary work done to date involves no stage beyond hydrogen and helium burning. There is only one primary product of hydrogen burning, ^{4}He. Clearly the next major burning stage after hydrogen burning must involve the consumption of ^{4}He. Since the energy generation rate for helium burning is fairly insensitive to the nature of the ashes formed, one can get through both hydrogen and helium burning with a rather crude treatment of nucleosynthesis, missing only some fairly subtle but conceptually important effects. However, if for example no ^{12}C is formed, then there is no carbon burning stage at all! This is a *qualitative* as well as a quantitative difference. For the later stages of stellar evolution it appears that the question of the composition produced as well as that of energy generation rate must be carefully considered.

Table I summarizes the primary thermonuclear burning stages in stars. Note that if a direct $e-\nu$ coupling in the weak interaction does exist, then stages after helium burning are dominated by neutrino cooling rather than photon diffusion.

There is one more point that should be stressed. Massive stars ($M \gtrsim 3M_\odot$) spend so little time in late burning stages (carbon burning and beyond) that the HR diagram is no longer such a useful test of evolutionary theory of these objects; this is due to poor statistics. However these stars all have a pronounced characteristic: they burn nuclear fuel at a prodigous rate. Their thermonuclear ashes may reveal their history.

TABLE I

Thermonuclear burning stages

Fuel	$T/10^9$ (K)	Ashes	q (ergs/g-fuel)	Cooling
^{1}H	0.02	^{4}He,^{14}N	$(5 \text{ to } 8) \times 10^{18}$	Photons
^{4}He	0.2	^{12}C, ^{16}O, ^{22}Ne	7×10^{17}	Photons
^{12}C	0.8	^{20}Ne, ^{24}Mg, ^{16}O;	5×10^{17}	Neutrinos
		^{23}Na, ^{25,26}Mg		Neutrinos
	0.4	^{20}Ne, ^{23}Na	–	Neutrinos
^{20}Ne	1.5	^{16}O, ^{24}Mg, ^{28}Si;	1.1×10^{17}	Neutrinos
^{16}O	2	^{28}Si, ^{32}S;	5×10^{17}	Neutrinos
^{28}Si	3.5	^{56}Ni, $A \sim 56$ Nuclei	$(0 \text{ to } 3) \times 10^{17}$	Neutrinos
^{56}Ni	6–10	n, ^{4}He, ^{1}H;	$\sim 8 \times 10^{18}$	Neutrinos
$A \sim 56$ Nuclei	(depends on ϱ)	photodisintegration and neutronization		

https://doi.org/10.1017/S0074180900017617 Published online by Cambridge University Press

In order to even attempt to read this history, and in a sense replace the HR diagram with an abundance table as our observational constraint, we must calculate abundances correctly.

3. Minimum Reaction Networks

The set of coupled nonlinear differential equations which govern abundances of nuclei undergoing thermonuclear reactions is referred to as a *reaction network*. As a star evolves to higher temperature and density an increase in the number of possible reactions results in more complex reaction networks. In principle all nuclei should be included in the reaction network. In practice the size of the network can be determined by an accuracy criterion (such as, all nuclei having abundances greater than ε are to be calculated to an accuracy of δ, where ε and δ are some chosen numbers). Clearly the accuracy needed depends upon the use to be made of the results. Con siderable computational economy can be obtained by judicious choice of the reaction network to be used. Consider all networks giving an error of size δ or less for any species having an abundance ε or greater. Any member of this set will be called an 'equivalent' network to any other member of the set. For efficiency we wish to find the minimum equivalent network, that is, the one with the fewest reactions and nuclear species. It should be noted that the question of accuracy will imply in practice the calibration of a smaller network by a larger, more general one.

Guided by these ideas I have developed what I consider to be the simplest acceptable network for helium and subsequent burning stages. The term 'acceptable' is a time dependent quantity; as we learn more we will require better treatments of the physics. The energy generation rate ε is well represented through oxygen burning; the composition for nuclei of abundance by mass of $\gtrsim 10\%$ is reasonably good up to the onset of oxygen burning. Beyond this point single nuclei are used to represent the Si to Ca and the Ti to Zn quasi equilibrium groups (denoted 'Si' and 'Ni' respectively). See Woosley *et al.* (1974) for details of how the nucleosynthesis actually occurs.

Table II lists the reactions which I now consider necessary to represent the helium, carbon, neon, oxygen and silicon burning stages. With the new evolutionary models now becoming available it should be possible to improve the silicon burning algorithm (although there is no evidence at present to indicate that the algorithm listed is inadequate). To better explain the approximations, Figure 2 presents the recommended groups of nuclei in a graphical format.

4. Helium Burning

As the first nuclear burning stage with more than one principal product, helium burning is a stage for which correct treatment of nucleosynthesis is vital. Renewed work on the triple-alpha reaction and especially new experimental work by Dyer (1973) at Caltech on $^{12}C(\alpha, \gamma)\,^{16}O$ has substantially improved the empirical basis of our helium burning calculations. Table III gives new rates suggested for these reactions. These expressions were derived from those given by Fowler *et al.* (1967 and private

https://doi.org/10.1017/S0074180900017617 Published online by Cambridge University Press

TABLE II

Minimum Reaction networks for energy generation

Fuel	Reactions
He	$3 \rightarrow {}^{12}C$
	${}^{12}C(\alpha, \gamma)\,{}^{16}O$
	${}^{16}O(\alpha, \gamma)\,{}^{20}Ne$ (small)
C	${}^{12}C({}^{12}C, \alpha)\,{}^{20}Ne$
	${}^{12}C({}^{12}C, p)\,{}^{23}Na\ (p, \alpha)\,{}^{20}Ne$
	${}^{16}O\ (\alpha, \gamma)\,{}^{20}Ne$
	${}^{20}Ne\ (\alpha, \gamma)\,{}^{24}Mg$
Ne	${}^{20}Ne\ (\gamma, \alpha)\,{}^{16}O$
	${}^{16}O\ (\gamma, \alpha)\ Ne^{20}$
	${}^{20}Ne\ (\alpha, \gamma)\,{}^{24}Mg$
	${}^{24}Mg\ (\alpha, \gamma)\,{}^{28}Si$ (small)
O	${}^{16}O\ ({}^{16}O, \alpha)\,{}^{28}Si$
	${}^{16}O\ ({}^{16}O, p)\,{}^{31}P\ (p, \gamma)\,{}^{28}Si$ etc.
	${}^{24}Mg\ (\alpha, \gamma)\,{}^{28}Si$
	${}^{28}Si + \alpha \rightarrow$ 'Si' = Si to Ca group
	ε is o.k. if we use ${}^{16}O$, ${}^{24}Mg$ and 'Si'
'Si'	'Si' $\rightarrow$ 'Ni' $\equiv A \sim 56$ nuclei
	as discussed by Bodansky *et al.* (1968)
	and Clayton (1968)

communication in August, 1973); the simplified expressions given here are valid *only* for hydrostatic helium burning temperatures. The ${}^{12}C(\alpha, \gamma)\,{}^{16}O$ rate reflects analysis of Dyer's data (by P. Dyer and by T. Tombrello) which attempts to abstract the contribution of the 7.115 MeV level in the ${}^{16}O$ compound nucleus from the laboratory measurement. The changes in the 3α rate and the ${}^{12}C(\alpha, \gamma)\,{}^{16}O$ rate are in different directions insofar as the nucleosynthesis of ${}^{12}C$ and ${}^{16}O$ is concerned. The change in the ${}^{12}C/{}^{16}O$ ratio in ashes of helium burning is therefore less than would be expected from either change taken alone. The reader should be warned that experiments currently underway and as yet unpublished may be reflected in further changes in these rates in the near future. Helium burning is one of the most difficult problems in experimental nuclear astrophysics; the current rate of progress in this area is exciting.

5. Carbon Burning

Recent experimental data on the ${}^{12}C + {}^{12}C$ reaction has been obtained at energies relevant to astrophysics by Patterson, Winkler, and Zaidins (1969, PWZ) and Mazarakis and Stephens (1972, 1973, MS). The Patterson *et al.* data went down to a center of mass energy of 3.25 MeV while that of Mazarakis and Stephens extended

https://doi.org/10.1017/S0074180900017617 Published online by Cambridge University Press

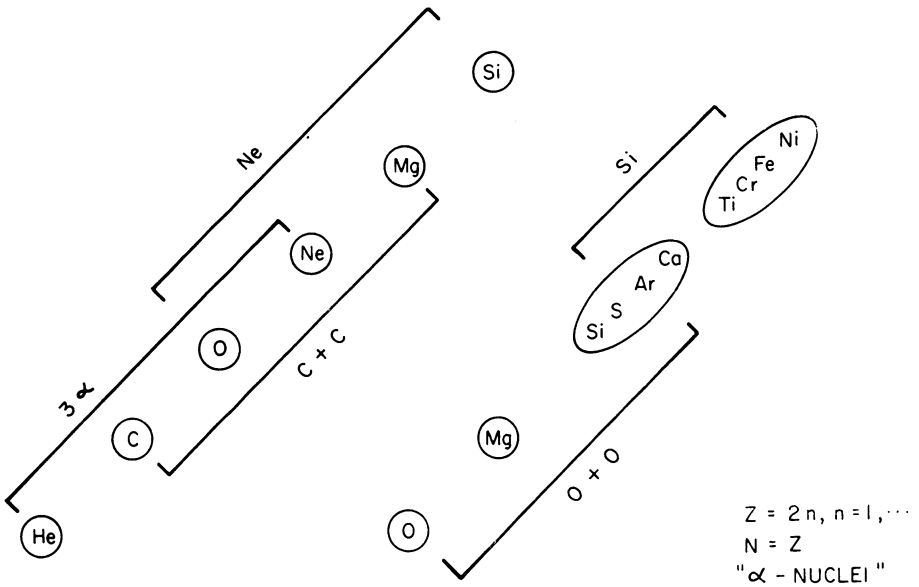

Fig. 2. Schematic diagram of groups of nuclei to be used for various burning stages.

TABLE III

New reaction rates for helium burning

$3\alpha \rightarrow {}^{12}C$. Fowler *et al.* (1967) and private communication (1973).
For $T_9 \sim 0.2$

$$a^2\langle\sigma v\rangle_{3\alpha} = \frac{1}{T_9^3}\,[2.48 \times 10^{-8} \exp(-4.4113/T_9) + 1.81 \times 10^{-8} \exp(-27.425/T_9)]$$

$$(\dot{Y}_c)_{3\alpha} = \varrho^2 Y_\alpha^3 a^2 \langle\sigma v\rangle_{3\alpha}/6;\quad Y_i \equiv X_i/A_i \equiv N_i/\varrho a$$

${}^{12}C(\alpha, \gamma){}^{16}O$. Same source. For $T_9 \sim 0.2$.

$$a\langle\sigma v\rangle_{12\alpha} = 6.87 \times 10^7 \exp(-32.12/T_9^{1/3})/T_9^2$$

down to 2.45 MeV. Since the optimum bombarding energy is

$$E_0 = 2.41\, T_9^{12/3}\ \text{MeV}$$

this corresponds to a temperature $T_9 \simeq 1$. The energy spread is

$$\Delta = 1.005\, T_9^{5/6}\ \text{MeV}.$$

These data are shown in Figure 3 in terms of the cross section factor

$$S = \sigma E\, e^{2\pi\eta},$$

https://doi.org/10.1017/S0074180900017617 Published online by Cambridge University Press

where σ is the cross section, E the center of mass energy, and $\eta = Z_1 Z_2 e^2/v$ is the Gamow factor for nuclei of proton number Z_1 and Z_2 with relative velocity v. The range of energy which determines the reaction rate is shown for $T_9 = 0.3$, 0.8 and 2.0. While the reaction rate is well determined for $T_9 = 2.0$ (i.e., explosive carbon burning), the rate is uncertain at $T_9 = 0.8$ and very uncertain at $T_9 = 0.3$. The early expression of Reeves (1966) is a fair average of the experimental data to date; it is shown as a solid curve. The fit of Patterson *et al.* (1969), shown as a dashed curve, represents their low energy data but not that of Mazarakis and Stephens (1972, 1973). If the rise in S at $E \simeq 2.5$ MeV is due to a resonant-like structure in the cross section, then the PWZ fit might be appropriate for lower energies. Michaud (1972) has discussed the experimental data in terms of an optical model; he suggests an increasing cross section factor with lower energy as shown by the dot-dashed curve.

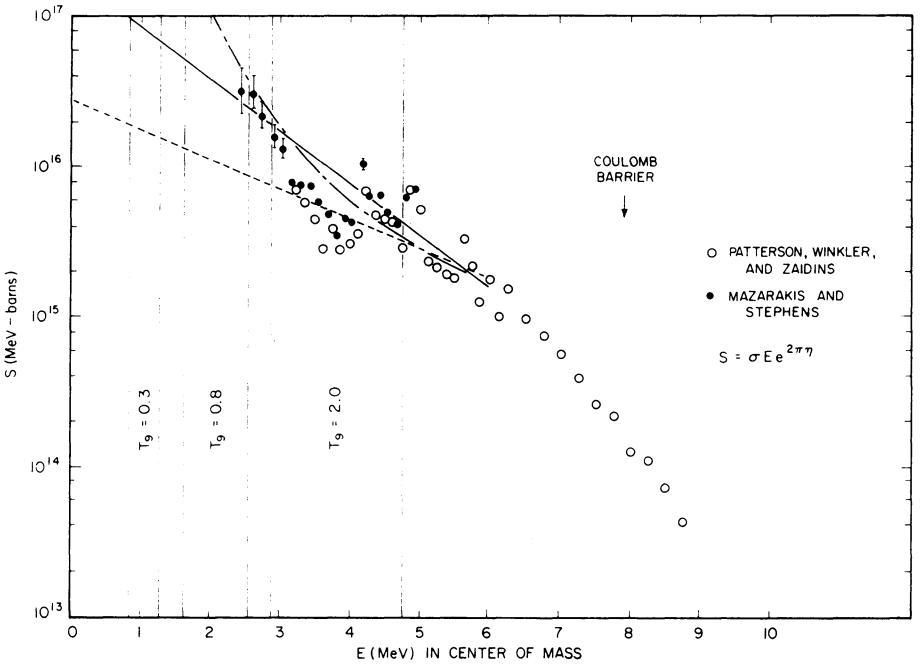

Fig. 3. Cross section factor for $^{12}C + ^{12}C$ as a function of center of mass energy.

Because the low energy measurements of $^{12}C + ^{12}C$ cross section have revealed unexpected phenomena, there is a fundamental uncertainty in the nuclear physics theory. This implies an uncertainty in which extrapolation method to use, and therefore an uncertainty in the $^{12}C + ^{12}C$ reaction below $E \simeq 2.5$ MeV. In view of this uncertainty three rates for $^{12}C + ^{12}C$ are listed in Table IV. Fortunately for $T_9 \gtrsim 0.8$ which is typical of hydrostatic carbon burning in most stars all three rates are fairly close in magnitude.

https://doi.org/10.1017/S0074180900017617 Published online by Cambridge University Press

TABLE IV

Reaction rates for $^{12}C + ^{12}C$

'Low':	Patterson *et al.* (1969)
	$a\langle\sigma v\rangle = T_9^{-2/3} \exp(61.053 - \tau)$
	$\tau = 84.173\,(1 + 0.0372\,T_9)^{1/3}/T_9^{1/3}$
'Middle':	Reeves (1966) (*Not* Reeves 1965!)
	$a\langle\sigma v\rangle = T_9^{-2/3} \exp(63.216 - \tau)$
	$\tau = 84.173\,(1 + 0.070\,T_9)^{1/3}/T_9^{1/3}$
'High':	Michaud (1972)
	$a\langle\sigma v\rangle = T_9^{-2/3} \exp(57.248 - 79.469/T_9^{1/3}), 0.3 \leqslant T_9 \leqslant 0.9$
	$= T_9^{-2/3} \exp(52.586 - 74.968/T_9^{1/3}), 0.9 \leqslant T_9 \leqslant 0.9$
	(The lower T expression has been slightly modified to fit more smoothly at $T_9 = 0.9$)

6. Neon and Oxygen Burning

The driving reaction for neon burning is $^{20}Ne(\gamma, \alpha)\,^{16}O$; at $T_9 \simeq 1.5$ its reaction rate has been reasonably well known for some time. Toevs *et al.* (1971) have recently reconfirmed the rate given earlier by Fowler *et al.* (1967). The reaction rates for the (α, γ) reactions on ^{16}O, ^{20}Ne and ^{24}Mg can be found in the latter reference and unpublished work by these authors (an updated review is planned). Table V gives the rate for $^{20}Ne(\gamma, \alpha)\,^{16}O$ for $T_9 \simeq 1.5$ and a fit to the $^{16}O + ^{16}O$ rate.

TABLE V

Some reaction rates for neon and oxygen burning

$^{20}Ne(\gamma, \alpha)\,^{16}O$.	Fowler *et al.* (1967) and Toevs *et al.* (1971)
	$\lambda_{\gamma,\alpha}(^{20}Ne) = 2.31 \times 10^{12} \exp(-65.247/T_9) +$
	$+ 2.21 \times 10^{13} \exp(-67.131/T_9)$
	For $T_9 \simeq 1.5$
$^{16}O + ^{16}O$.	A fit to the data of Spinka and Winkler (1972)
	$a\langle\sigma v\rangle = T_9^{-2/3} \exp(86.338 - \tau)$
	$\tau = 135.958(1 + 0.053\,T_9)^{1/3}/T_9^{1/3}$

Before discussing the $^{16}O + ^{16}O$ reaction it is enlightening to consider $^{12}C + ^{16}O$ (Figure 4) and then compare these as well as $^{12}C + ^{12}C$. The behavior of the cross section factor for $^{12}C + ^{16}O$ as taken from the data of Patterson *et al.* (1971) and of Kuehner and Almqvist (1964). The solid curve is the fit of Woosley *et al.* (1971), which is very similar to that of Michaud (1972). Although the fine scale resonant structure is not seen, a large scale resonant 'hump' at $E \simeq 6.5$ MeV appears which is not unlike that seen in $^{12}C + ^{12}C$ at $E \simeq 4.7$ MeV or so (see Figure 3). In Figure 5 is shown the data of Spinka and Winkler (1972) for the $^{16}O + ^{16}O$ reaction. This is a particularly difficult reaction from the experimental point of view because of the many possible exit channels. In analogy with $^{12}C + ^{12}C$ and $^{12}C + ^{16}O$ one might suspect

https://doi.org/10.1017/S0074180900017617 Published online by Cambridge University Press

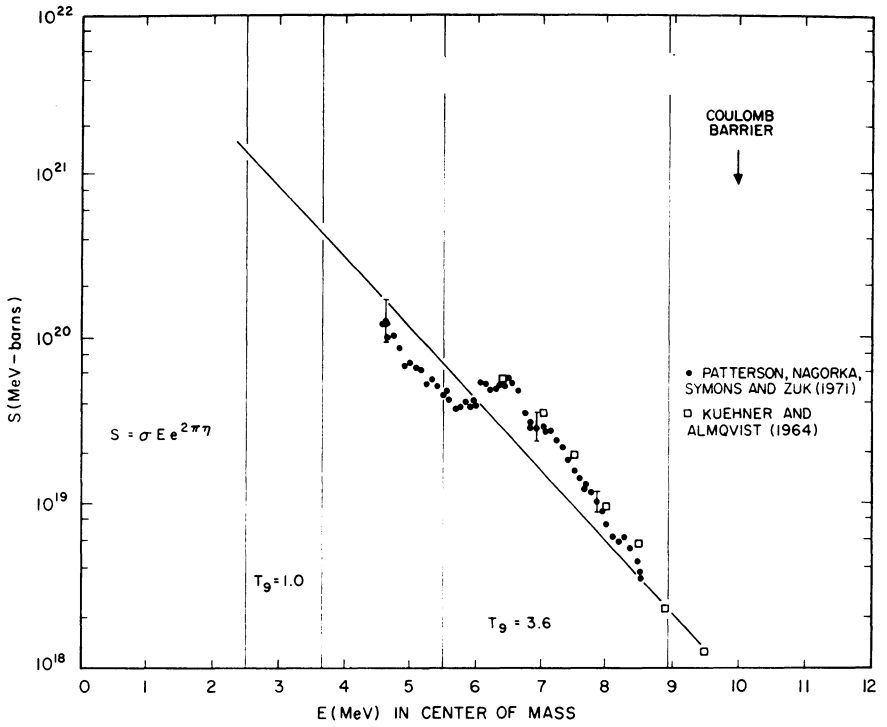

Fig. 4. Cross section factor for $^{12}C + ^{16}O$ as a function of center of mass energy.

that the experimental results extend down to the region of the 'hump', and that S will increase again from 6 to 4 MeV. This is merely a speculation.

Reeves (1965) used the higher energy data then available (unfortunately it was meager) to obtain the rate illustrated by the dotted line. This is most probably a severe overestimate at hydrostatic oxygen burning temperatures; use of this rate is *not* recommended. The dashed line presents the expression of Fowler and Hoyle (1964), which has also been widely used, for comparison. The recommended rate is the dot-dashed line (see Table V). This has the same slope as the expression of Truran and Arnett (1970) but is lower by about a factor of two. Michaud (1972) gets an expression which is virtually identical to this new rate except that it also should be reduced by a factor of two to account for a recalibration of the Spinka-Winkler data just prior to publication.

7. Some Structural Effects

The particular nature of the neutrino emission (as predicted for example by the conserved vector current theory) and of the nuclear energy generation causes some important structural changes in the late stages of stellar evolution. A detailed analysis of some of these effects has been published (Arnett, 1972).

https://doi.org/10.1017/S0074180900017617 Published online by Cambridge University Press

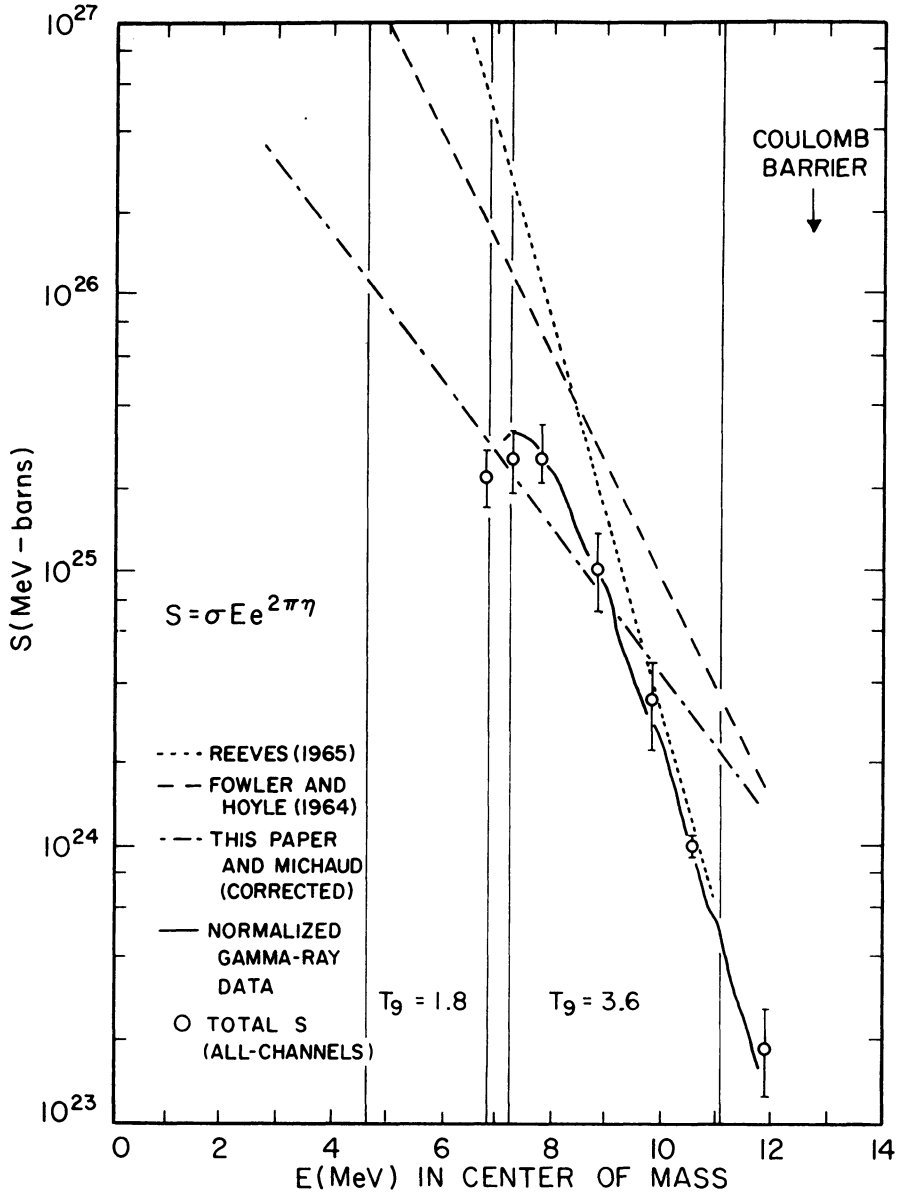

Fig. 5. Cross section factor for $^{16}O + {}^{16}O$ as a function of center mass energy (Spinka and Winkler, 1972).

(A) Energy loss by neutrinos due to a direct $e-\nu$ coupling is a local process, determined by the local temperature and electron number density. If we approximate this energy loss (per gram) by

$$\varepsilon_\nu \propto T^k$$

https://doi.org/10.1017/S0074180900017617 Published online by Cambridge University Press

then $k \gg 1$. Since the internal energy of matter in the relevant range of temperature T and density ϱ is roughly $E \propto T$, the hot inner regions of a star encounter the most severe cooling. Before a nuclear fuel ignites the only energy source is gravitational contraction, but this rate of energy supply is proportional to the local compression. For homologous contraction the fractional rate of energy supply is uniform. The central regions show a marked tendency to establish an isothermal temperature structure because the outlying layers show a larger fraction temperature increase than the inner layers. A strong, positive entropy gradient develops between the inner and outer regions.

(B) If we approximate the nuclear energy generation rate by

$$\varepsilon \propto T^m,$$

then $m > k \gg 1$. There is a critical temperature $T = T_{\text{crit}}$ at which $\varepsilon - \varepsilon_\nu = 0$. For $T > T_{\text{crit}}$ the nuclear rate dominates and heating occurs (in the absence of rapid expansion); similarly for $T < T_{\text{crit}}$ the neutrino rate dominates and cooling occurs (in the absence of rapid contraction). Suppose $T > T_{\text{crit}}$, so that nuclear energy is rapidly released. If photon diffusion and electron conduction of heat are ineffective (roughly $T \gtrsim 0.5 \times$ $\times 10^9$ K) then the nuclear energy goes into heating and expanding the matter. Convective instability develops, and the hot buoyant blob floats upward, transporting energy, expanding and cooling.

(C) Consider the thermal balance for the convective core. Note that since $m > k$ the nuclear energy release is more concentrated toward the region of highest temperature (the centre of the star if the matter is not highly degenerate). If the mass contained in the convective core M_{cc} is small, then

$$\int_0^{M_{cc}} \varepsilon \, \mathrm{d}m > \int_0^{M_{cc}} \varepsilon_\nu \, \mathrm{d}m$$

and the entropy of the core increases. This allows the core to grow, enclosing more mass, until

$$\int_0^{M_{cc}} \varepsilon \, \mathrm{d}m = \int_0^{M_{cc}} \varepsilon_\nu \, \mathrm{d}m .$$

Note that this does *not* imply thermal equilibrium for the star as a whole, i.e.,

$$\int_0^{M} \varepsilon \, \mathrm{d}m \neq \int_0^{M} \varepsilon_\nu \, \mathrm{d}m$$

in general. Neglect of this latter point is probably the cause of some controversy with regard to analysis of the pulsational stability of these objects.

(D) The conditions above give rise to a phenomenon of 'core-size reduction'. For each successive stage the mass converted to 'ashes' is a small fraction of that potentially available as 'fuel'. The core gets smaller with each stage, and is surrounded by a

https://doi.org/10.1017/S0074180900017617 Published online by Cambridge University Press

growing mantle of unburned fuel. How small can the core – that is the central region which has undergone the most advanced burning – actually get? If its mass is less than about 1.4 $M_\odot$ (the Chandrasekhar limit, roughly speaking) it can support itself by its electron degeneracy pressure. Such a core does not contract and heat up to ignite the next burning stage. We have a 'waiting point'. The core is separated from the fuel of the last burning stage by a shell burning that fuel. If this burning increases the core mass then the core mass eventually rises to $M \gtrsim 1.4\ M_\odot$, contraction, heating and ignition of the next burning stage can occur.

These processes are vital to our understanding of nucleosynthesis, presupernovae and gravitational collapse. It appears that the physical processes occurring in advanced evolution of stars set the stage in a very particular way for the stellar death scene.

8. Results of Some Recent Evolutionary Calculations Using These Rates

How do these topics relate to actual evolutionary calculations of stars? Table VI summarizes some aspects of a set of evolutionary calculations of helium stars of mass $M_\alpha = 4$, 8, 16, 32, 64, and 100 $M_\odot$. These may be thought of as helium cores enclosed in a hydrogen rich envelope (corresponding masses are given in Table VI as $M/M_\odot$), or as stars which have lost their hydrogen rich envelope as probably would occur for example in a close binary system. The most massive objects ($M_\alpha = 64$ and 100 $M_\odot$) became unstable to the electron-pair instability ($\gamma < \frac{4}{3}$ because of copious $e^\pm$ production). The lower masses (which are probably the astronomically relevant ones)

TABLE VI

Summary of the calculations for various helium core masses M_α (Abundances are by mass)

$M_\alpha/M_\odot$	4	8	16	32	64[b]	100[b]	Solar system	Galactic cosmic rays
$M/M_\odot$	15	22	36	70	120	170	–	–
He/O	11	1.9	.66	.41	.12	.16	25.0	7.3
C/O	1.1	.35	.21	.17	.070	.039	0.41	0.71
Ne/O	.23	.46	.33	.091	.014	.0071	0.20	0.24
Mg/O	.41	.15	.10	.047	.056	.044	0.075	0.33
Si/O[c]	7.2[a]	.28[a]	.055[a]	.073[a]	.095	.72	0.082	0.33
Fe/O[d]	2.1[a]	.80[a]	.24[a]	.14[a]	0.	.25	0.140	0.76
Stage	Core Si flash	Core Si flash	Core collapse	Core collapse	Post explosion	Post explosion	–	–
Central core mass/$M_\odot$	~ 1.4	~ 1.4	~ 1.4	~ 1.4	2.2 $M_\odot$ (Si) remnant	No remnant	–	–

[a] Will be significantly modified by remnant formation and explosive processing.
[b] Abundances in ejected matter only.
[c] Si refers to the quasi equilibrium cluster from Si through Ca.
[d] Fe refers to the quasi equilibrium cluster around $A = 56$ (the 'iron' peak).

https://doi.org/10.1017/S0074180900017617 Published online by Cambridge University Press

all evolved to core collapse with nearly identical core structure and mass ($M_{\text{core}} \simeq$ $\simeq 1.4\ M_\odot$ of iron group elements).

The abundances of ^{4}He, ^{12}C, ^{20}Ne, ^{24}Mg as well as the 'Si' and the 'Fe' (or 'Ni') quasi equilibrium groups are tabulated, relative to ^{16}O, for all M_α. If each core becomes a neutron star (at least in a statistical sense), and each neutron star thus formed accelerates an equal number of the surrounding nuclei to cosmic ray energies, the resulting abundance distribution agrees well with the observed abundance distribution for galactic cosmic rays. (This number average abundance distribution is close to that shown for $M_\alpha = 4\ M_\odot$; compare with the column in Table VI called 'Galactic Cosmic Rays'). Even the curious C/O ratio in the cosmic rays appears naturally. See Arnett and Schramm (1973) for more details.

Similarly, if we do a mass average of $M_\alpha = 4, 8, 16, 32\ M_\odot$ ($M = 15, 22, 36$ and $70\ M_\odot$) over a realistic initial mass function then the resulting abundances agree with the 'cosmic' (solar system) abundances for C, O, Ne and Mg to within a factor of two. If we assume the remnant mass (in a statistical sense) is $\sim 1.4\ M_\odot$, then the abundance of Si + Fe is about right also. If we use even modestly realistic models of galactic evolution we find that the absolute as well as the relative abundance of these elements are correctly predicted.

These results are startling. The calculations are more than sufficiently general to allow widely divergent abundance distributions to appear. This may be an important clue as to the nature of the late stages of stellar evolution. By such abundance arguments we may learn something about gravitational collapse as well as nucleosynthesis and the late stages of stellar evolution.

Acknowledgement

The assistance of the National Science Foundation and the National Academy of Sciences is gratefully acknowledged.

References

Arnett, W. D.: 1972, *Astrophys. J.* **173**, 393.
Arnett, W. D.: 1974, *Thermonuclear Evolution of Stars and Galaxies*, Univ. of Chicago Press, Chicago.
Arnett, W. D. and Schramm, D. N.: 1973, *Astrophys. J.* **185**, L47.
Beaudet, G., Petrosian, V., and Salpeter, E. E.: 1967, *Astrophys. J.* **150**, 979.
Bodansky, D., Clayton, D. D., and Fowler, W. A.: 1968, *Astrophys. J. Suppl.* **16**, 299.
Clayton, D. D.: 1968, *Principles of Stellar Evolution and Nucleosynthesis* (McGraw-Hill: New York).
Dicus, D,: 1972, *Phys. Rev.* **D6**, 941.
Dyer, P.: 1973, in D. N. Schramm and W. D. Arnett (eds.), *Explosive Nucleosynthesis*, Univ. of Texas Press, Austin, p. 195.
Festa, G. C. and Ruderman, M. A.: 1969, *Phys. Rev.* **180**, 1227.
Feynman, R. P. and Gell-Mann, M.: 1958, *Phys. Rev.* **109**, 193.
Fowler, W. A., Caughlan, G., and Zimmerman, B. A.: 1967, *Ann. Rev. Astron. Astrophys.* **5**, 525.
Fowler, W. A. and Hoyle, F.: 1964, *Astrophys. J. Suppl.* **9**, 201.
Kuehner, J. A. and Almqvist, E.: 1964, *Phys. Rev.* **134**, B1229.
Mazarakis, M. and Stephens, W.: 1972, *Astrophys. J. Letters* **171**, L97.
Mazarakis, M. and Stephens, W.: 1973, *Phys. Rev.* C7, 1280.

https://doi.org/10.1017/S0074180900017617 Published online by Cambridge University Press

Michaud, G.: 1972, *Astrophys. J.* **175**, 751.
Patterson, J. R., Nagorka, B. N., Symons, G., and Zuk, W. M.: 1971, *Nucl. Phys.* **A164**, 545.
Patterson, J. R., Winkler, H., and Zaidins, C.: 1969, *Astrophys. J.* **157**, 367.
Pontecorvo, B.: 1959, *Zh. Eksper. Teor. Fiz.* **36**, 615; 1960 *Soviet Phys. JETP* **9**, 1148.
Reeves, H.: 1965, *Stars and Stellar Systems* **8**, 113.
Reeves, H.: 1966, *Astrophys. J.* **146**, 447.
Spinka, H. and Winkler, H.: 1972, *Astrophys. J.* **174**, 455.
Toevs, J. W., Fowler, W. A., Barnes, C. A., and Lyons, P.: 1971, *Astrophys. J.* **169**, 421.
Truran, J. W. and Arnett, W. D.: 1970, *Astrophys. J.* **160**, 181.
Weinberg, S.: 1971, *Phys. Rev. Letters* **27**, 1688.
Woosley, S. E., Arnett, W. D., and Clayton, D. D.: 1971, *Phys. Rev. Letters* **27**, 213.
Woosley, S. E., Arnett, W. D., and Clayton, D. D.: 1974, *Astrophys. J. Suppl.* **26**, 231.

https://doi.org/10.1017/S0074180900017617 Published online by Cambridge University Press